Inorg. Chem. **2003**, *42*, 4006–4017

Spectroscopic Characterization of the Leu513His Variant of Fungal Laccase: Effect of Increased Axial Ligand Interaction on the Geometric and Electronic Structure of the Type 1 Cu Site

Amy E. Palmer,[†] Robert K. Szilagyi,[†] Joel R. Cherry,[‡] Aubrey Jones,[‡] Feng Xu,*[,‡] and Edward I. Solomon*[,†]

Department of Chemistry, Stanford University, Stanford, California 94305 and Novozymes Biotech, Davis, California 95616

Received October 9, 2002

A variety of spectroscopic techniques, combined with density functional calculations, are used to describe the electronic structure of the Leu513His variant of the type 1 Cu site in *Myceliophthora thermophila* laccase. This mutation changes the type 1 Cu from a blue to a green site. Electron paramagnetic resonance (EPR), optical absorption, circular dichroism, and magnetic circular dichroism (MCD) spectroscopies reveal that, relative to the trigonal planar blue type 1 Cu site in wild-type fungal laccase, the covalency and the ligand field strength at the Leu513His green type 1 Cu center decrease. Additionally, there is a significant reorientation of the $d_{x^2-y^2}$ singly occupied MO, such that the overlap with the Cys sulfur valence orbital changes from π to σ. A density functional study in which internal coordinates are systematically altered reveals that these changes are due to the increased strength of the axial ligand (none to His), leading to a tetragonal distortion and elongation of the equatorial Cu-ligand bonds. These calculations provide insight into the experimental differences in the EPR parameters, charge-transfer absorption spectrum, and ligand-field MCD spectrum between the axial-His variant and blue Cu centers (plastocyanin and the type 1 site in fungal laccase). There are also significant differences between the green site in the Leu513His variant and other naturally occurring, green type 1 Cu sites such as in nitrite reductase, which have short axial Cu–S(Met) bonds. The large difference in EPR parameters between these green type 1 sites derives from a change in ligand field excitation energies observed by MCD, which reflects a decrease in ligand field strength. This is associated with different steric interactions of a His vs an axial Met ligand in a tetragonally distorted type 1 site. Changes in the electronic structure of the Cu site correlate with the difference in reactivity of the green His variant relative to blue wild-type fungal laccase.

Introduction

Laccase (*p*-diphenol: dioxygen oxidoreductase, EC 1.10.3.2) belongs to the family of multicopper oxidases, which utilize four copper ions to couple four one-electron substrate oxidations with the four-electron reduction of dioxygen to water.[1,2] The different Cu sites are classified into three types based on the spectroscopic properties they exhibit in the oxidized (Cu^{2+}) state. The type 1 (T1), or blue, Cu site is characterized by an intense ($\epsilon \approx 5000\ M^{-1}\ cm^{-1}$) absorption feature around 600 nm and small ($<100 \times 10^{-4}\ cm^{-1}$) parallel hyperfine coupling in electron paramagnetic resonance (EPR). These unusual spectroscopic features are due to a highly covalent π bond between the S(Cys) and the Cu^{2+}. The type 2 (T2), or normal, Cu site displays parallel hyperfine coupling ($>160 \times 10^{-4}\ cm^{-1}$) typical of normal tetragonal Cu and does not exhibit intense features in the visible absorption or circular dichroism (CD) spectrum. Finally, the type 3 (T3), or coupled binuclear, Cu site is comprised of two Cu^{2+} ions which are antiferromagnetically coupled through a bridging hydroxide.[3] The resulting dia-

* Authors to whom correspondence should be addressed. E-mail: Edward.Solomon@Stanford.edu (E.I.S.); fxu@novozymesbiotech.com (F.X.).
[†] Stanford University.
[‡] Novozymes Biotech.

(1) Solomon, E. I.; Sundaram, U. M.; Machonkin, T. E. *Chem. Rev.* **1996**, *96*, 2563−2605.
(2) Solomon, E. I.; Chen, P.; Lee, S. K.; Metz, M.; Palmer, A. E. *Angew. Chem. Int. Ed.* **2001**, *40*, 4570−4590.
(3) Messerschmidt, A.; Ladenstein, R.; Huber, R.; Bolognesi, M.; Avigliano, L.; Petruzzelli, R.; Rossi, A.; Finazzi-Agró, A. *J. Mol. Biol.* **1992**, *224*, 179−205.

10.1021/ic026099n CCC: $25.00
Published on Web 06/05/2003

magnetic ($S_{total} = 0$) T3 Cu site lacks an EPR signal, but displays an absorption feature around 330 nm ($\epsilon \approx 5000$ M^{-1} cm^{-1}). In fungal laccase, the T2 and T3 sites are within 4 Å of each other and together form a trinuclear Cu cluster, which is the site of O_2 reduction. The T1 Cu site shuttles electrons from substrate, typically diphenols, aryl diamines, or amino phenols, to the T2/T3 trinuclear Cu cluster.[1]

The T1 Cu site of fungal laccase is an unusual blue Cu site because it lacks an axial ligand, rendering the site trigonal planar. Previous spectroscopic studies[4] on the T1 Cu site from three different wild-type fungal laccases (*Polyporus pinsitis* (PpL), *Rhizoctonia solani* (RsL), and *Myceliophthora thermophila* (MtL)) revealed that this T1 Cu site is characterized by increased covalency of the Cu−S(Cys) π bond and increased strength of the ligand field as compared to the classic T1 site in plastocyanin, which has an axial Met ligand.[4] Both of these changes were found to be derived from the lack of the axial ligand. Additionally, investigations on a variant of PpL, in which the "axial" noncoordinating Leu463 was changed to a weakly coordinating Met (L463M PpL) confirmed that the T1 Cu axial ligand environment played a role in tuning the covalency, geometry, and electronic structure of the site.[4]

Extensive studies on other blue Cu proteins have focused on the T1 Cu ligand environment and how it impacts the electronic properties of the Cu site. A number of proteins with "perturbed" T1 sites are actually green rather than blue in color. These sites exist naturally in proteins such as nitrite reductase (NiR)[5,6] and cucumber basic protein (CBP),[7,8] which have a short, axial Cu−S(Met) bond and have been engineered into classic blue Cu sites such as the Met121 to His variant of azurin from *Alcaligenes denitrificans*[9] (M121H A.d. azurin). The electronic structure of the green T1 sites in NiR and CBP differs significantly from that of classic blue Cu sites. Relative to plastocyanin, the green T1 Cu sites in NiR and CBP exhibit an increased ligand field and a rotation of the singly occupied Cu $d_{x^2-y^2}$ HOMO, which increases the pseudo-σ and decreases the π interaction of the S(Cys) with the Cu.[10,11] These electronic structure changes have been correlated with a shorter Cu−S(Met) bond, which results in an increased Jahn−Teller distorting force and leads to a more flattened, tetragonal geometry.

In M121H A.d. azurin, absorption, EPR, resonance Raman, and X-ray crystal structural studies reveal perturbation of the T1 Cu site upon mutation of the axial-Met to His.[9,12,13] In particular, the Cys → Cu charge-transfer transition at 600 nm shifts to higher energy and the ν(Cu−S(Cys)) envelope in resonance Raman moves to a lower Raman shift, indicating a weaker Cu−S(Cys) bond. However, a detailed description of the electronic structure of this variant and its relation to other green Cu sites has not been conducted. One complication of M121H A.d. azurin is that it undergoes a significant change upon lowering the pH. Spectroscopic and X-ray crystallographic studies reveal that the N_δ of axial-His121 protonates at low pH and dissociates from the oxidized Cu, resulting in a T1 blue Cu site. The authors implicate a trans-axial Gly45 and hydrogen bonding between His121 and Ser9 as potentially playing a role in this pH dependence. An additional difficulty of the M121H A.d. azurin variant is that even at high pH (pH 7−10.5), a fraction of the protein (~25%) exhibits characteristics of a blue T1 Cu site and therefore all protein samples contain a mixture of species.[9]

This study presents the spectroscopic characterization of a variant of *Myceliophthora thermophila* laccase in which the noncoordinating "axial" Leu513 is replaced with His. This mutation causes the protein to change from blue to green, indicating a significant perturbation of the T1 site. In contrast to the M121H azurin variant, the spectroscopic properties of this new fungal laccase variant are not affected by pH. In addition, the T1 Cu site exists as a single species, and therefore the combination of absorption, CD, and magnetic circular dichroism (MCD) spectroscopy allows a detailed description of the ligand field of this axial-His variant for the first time. Additionally, spectroscopically adjusted density functional (DFT) calculations were carried out to gain further insight into the electronic structure of the ground state. The combination of experimental data and DFT calculations allows a comparison of the electronic structure of the axial-His variant with traditional blue Cu sites and other green Cu sites.

Materials and Methods

Preparation of MtL Variants. The protocols for molecular biology experiments (including restriction digests, DNA ligations, gel electrophoresis, and DNA preparations) were adapted from either the instructions of the manufacturer or standard procedures. Oligonucleotides were synthesized using an Applied Biosystems 294 DNA/RNA synthesizer. Nucleotide sequences were determined by an Applied Biosystems 373A-1.2.0 DNA sequencer. The plasmid construction, transformation, and fermentation were similar to those described previously.[14,15] Briefly, a plasmid pAJ032 was constructed from pRaMB17. A fragment encoding the T1 Cu-ligating peptide

(4) Palmer, A. E.; Randall, D. W.; Xu, F.; Solomon, E. I. *J. Am. Chem. Soc.* **1999**, *121*, 7138−7149.
(5) Iwasaki, H.; Noji, S.; Shidara, S. *J. Biochem.* **1975**, *78*, 355−361.
(6) Liu, M.-Y.; Liu, M.-C.; Payne, W. J.; LeGall, J. *J. Bacteriol.* **1986**, *166*, 604−608.
(7) Aikazyan, V. T.; Nalbandyan, R. M. *FEBS Lett.* **1975**, *55*, 272−274.
(8) Sakurai, T.; Okamoto, H.; Kawahara, K.; Nakahara, A. *FEBS Lett.* **1982**, *147*, 220−224.
(9) Kroes, S. J.; Hoitink, C. W. G.; Andrew, C. R.; Ai, J.; Sanders-Loehr, J.; Messerschmidt, A.; Hagen, W. R.; Canters, G. W. *Eur. J. Biochem.* **1996**, *240*, 342−351.
(10) LaCroix, L. B.; Shadle, S. E.; Wang, Y.; Averill, B. A.; Hedman, B.; Hodgson, K. O.; Solomon, E. I. *J. Am. Chem. Soc.* **1996**, *118*, 7755−7768.
(11) LaCroix, L. B.; Randall, D. W.; Nersissian, A. M.; Hoitink, C. W. G.; Canters, G. W.; Valentine, J. S.; Solomon, E. I. *J. Am. Chem. Soc.* **1998**, *120*, 9621−9631.
(12) Messerschmidt, A.; Prade, L.; Kroes, S. J.; Sanders-Loehr, J.; Huber, R.; Canters, G. W. *Proc. Natl. Acad. Sci. U.S.A.* **1998**, *95*, 3443−3448.
(13) van Gastel, M.; Canters, G. W.; Krupka, H.; Messerschmidt, A.; de Waal, E. C.; Warmerdam, G. C. M.; Groenen, E. J. J. *J. Am. Chem. Soc.* **2000**, *122*, 2322−2328.
(14) Xu, F.; Berka, R. M.; Wahleithner, J. A.; Nelson, B. A.; Shuster, J. R.; Brown, S. H.; Palmer, A. E.; Solomon, E. I. *Biochem. J.* **1998**, *334*, 63−70.
(15) Berka, R. M.; Schneider, P.; Golightly, E. J.; Brown, S. H.; Madden, M. S.; Brown, K. M.; Halkier, T.; Mondorf, K.; Xu, F. *Appl. Environ. Microbiol.* **1997**, *63*, 3151−3157.

segment of MtL was subcloned into pUC118, from which single-stranded DNA was prepared and used as a template for site-directed mutagenesis with the primers 5′dACATCGCCTGGCACGTCTCGGGTGGACATGGCGTC GTCTACCTCG3′ (for Leu513His variant), 5′dACATCGCCTGGCTCGTCTCGGGTGGAC ATGGCGTCGTCTACCTC G3′ (for His508Leu and Leu513His variants), 5′dCTGGCTGTTC CACTCCCACATCGCCT3′ (for Cys503Ser variants), and 5′dCTGGCTGTTCCACCACCAT CGCCTGGCTGCGTCTCGGGCGGCCTGGG3′ (for Cys503His and His508Cys variants). The variants were identified by hybridization with the corresponding radio-labeled oligonucleotide primer and verified by DNA sequence analysis. The DNA segments encoding MtL variants were subcloned into a vector containing *Aspergillus niger* NA2-tpi promoter, AMG terminator, and *amdS* gene. The subcloned variants were transformed into *A. oryzae* as previously described,[14] except that 1 cm^3 of SPTC (0.8 M sorbitol, 40% poly(ethylene glycol) 4000 [BDH], 50 mM Tris-HCl, pH 8.0, 50 mM $CaCl_2$) was used instead of the PEG solution. Plated on Cove medium containing 5 mM ABTS, active transformants were selected, spore-purified, and fermented in 125 cm^3 shake flasks for 5 days at 34 °C. Only the Leu513His variant showed significant expression in shake flask and was fermented in a 10-L fermentor for purification and characterization. The purification was similar to that previously described,[14] with a recovery yield of 40%.

Enzyme Characterization. The enzyme concentration was determined using the absorption band at 280 nm ($\epsilon_{280} = 146\ mM^{-1}\ cm^{-1}$). The molar absorptivity (ϵ) at 280 nm was determined by amino acid analysis. Laccase-catalyzed oxidation of syringaldazine (SGZ), methyl syringate (MS), or 2,2′-azinobis-(3-ethylbenzothiazoline-6-sulfonic acid) (ABTS) and kinetic analysis were performed as previously reported.[16] Copper concentrations were determined spectrophotometrically using 2,2′-biquinoline[17] or by atomic absorption spectroscopy. The amount of reduced Cu was determined using the modified 2,2′-biquinoline assay.[18] The concentration of paramagnetic Cu was determined from spin quantitation of EPR spectra (vide infra). Spectra were normalized to Cu^{2+} concentration. Experiments on the pH dependence of the activity profile used Britton and Robinson (B&R) buffer (pH 2.7−11, made by mixing 0.1 M boric acid, 0.1 M acetic acid, and 0.1 M phosphoric acid with 0.5 M NaOH to desired pH). All spectroscopic experiments were performed in 100 mM potassium phosphate buffer, pH = 6 (pD = 6.0 for MCD experiments). The reduction potential of the T1 Cu in L513H MtL in 10 mM phosphate buffer, pH 7.0, was obtained by the poised potential method. To 0.2 mM of degassed protein, were anaerobically added aliquots of $K_4[Fe(CN)_6]$ (0.0−33.3 mM) to a final concentration of 50 mM, and the absorption spectrum was monitored until equilibrium was achieved for each titration point. Chemicals used as buffers were reagent grade and were used without further purification. Water was purified to a resistivity of 15−18 MΩ using a Barnstead Nanopure deionizing system.

Spectroscopic Studies. EPR spectra were obtained using a Bruker ER 220D-SRC spectrometer. All samples were run at 77 K in a liquid nitrogen finger Dewar. EPR spectra were spin-quantitated using a Cu standard, $Cu(ClO_4)_2$,[19] of known concentration run in the same tube as the sample. Simulations of EPR spectra were performed using the program SIM15.[20] Room-temperature UV−visible absorption spectra were obtained using either a Hewlett-Packard HP8452A diode array or a Shimadzu UV160LI spectrophotometer. Room-temperature CD and low-temperature (5 K) MCD spectra in the 300−800 nm region were collected with a Jasco J-500-C spectropolarimeter operating with an S-20 photomultiplier tube and an Oxford SM4-7T magnet. CD and MCD spectra in the 700−2000 nm region were recorded with a Jasco J-200-D spectropolarimeter, a liquid nitrogen cooled InSb detector, and an Oxford SM4000-7T magnet. CD samples were run in a 1.0 cm quartz cuvette. MCD samples were run in MCD cells fitted with quartz disks and a 0.3 cm rubber gasket spacer. Simultaneous Gaussian fitting of the absorption, CD, and MCD spectra was performed using the PeakFit program (Jandel).[21]

Electronic Structure Calculations. Gradient-corrected density functional calculations (GGA-DFT) were carried out using ADF2001[22−25] on a 40-cpu heterogeneous cluster of SGI Origin, IBM RISC, and IBM PC compatible computers. The Becke88 exchange[26] and Perdew86[27] correlation nonlocal functionals were used with Wosko−Vilk−Nussair local functionals[28] as implemented in the software package (BP86). The triple-ζ quality, Slater-type all-electron basis set (BSIV[29]) was employed with a single polarization function. This basis set has previously been shown to be theoretically converged for Cu-containing systems,[30] and additional polarization functions (BSV) do not improve the electronic structure description. Because the standard GGA-DFT calculations give too much ligand character in the ground-state wave function compared to the experiment, the nuclear charge of the Cu was reduced by 0.45e, giving a reasonable bonding description as discussed for other cupric systems.[31]

The active-site models were constructed from imidazole, methyl thiolate, and dimethyl thioether molecules. The atomic coordinates of the blue Cu-based geometries were taken from the 1.33 Å resolution X-ray structure of the Poplar plastocyanin (Plc).[32] Because there is no structural data for the L513H laccase variant, the atomic coordinates of the axial-His variant models were taken from the 1.89 Å resolution, room temperature (RT models) and from the 1.91 Å resolution, liquid nitrogen temperature X-ray structures (LT models) of the M121H A.d. azurin at pH 6.5 (referred to high pH forms in ref 12). Each crystal structure contains two, crystallographically independent active sites, which are virtually identical within the resolution of 1.9 Å. Instead of using a hypothetical, averaged geometry, the experimental structures of the four active sites were employed to take into account possible variations in the calculated ground- and excited-state properties due to structural differences[33] (vide infra). Single-point energy calculations were performed without symmetry constraints.

(16) Xu, F. *Biochemistry* **1996**, *35*, 7608−7614.
(17) Felsenfeld, G. *Arch. Biochem. Biophys.* **1960**, *87*, 247−251.
(18) Hanna, P. M.; Tamilarasan, R.; McMillin, D. R. *Biochem. J.* **1988**, *256*, 1001−1004.
(19) Carithers, R. P.; Palmer, G. *J. Biol. Chem.* **1981**, *256*, 7967−7976.
(20) Lozos, G. P.; Hoffman, B. M.; Franz, C. G. *QCPE Bull.: QCPE program number QCMP155* **1974**, *11*.
(21) *PeakFit* version 4.06; SPSS, Inc., AISN Software, Inc., 1995.
(22) Baerends, E. J. E.; Ellis, D. E.; Ros, P. D. *Chem. Phys.* **1973**, *2*, 41−51.
(23) Versluis, L. Z.; Ziegler, T. *J. Chem. Phys.* **1988**, *88*, 322−328.
(24) teVelde, G.; Baerends, E. J. *J. Comput. Phys.* **1992**, *99*, 84−98.
(25) Guerra, C. F.; Snijders, J. G.; teVelde, G.; Baerends, E. J. *Theor. Chem. Acc.* **1998**, *99*, 391−403.
(26) Becke, A. D. *Phys. Rev. A: At., Mol., Opt. Phys.* **1988**, *38*.
(27) Perdew, J. P. *Phys. Rev. B: Condens. Matter Mater. Phys.* **1986**, *33*.
(28) Vosko, S. H.; Wilk, L.; Nusair, M. *Can. J. Phys.* **1980**, *58*, 8.
(29) *Amsterdam Density Functional*, 1st ed.; Scientific Computing and Modelling NV: Amsterdam, The Netherlands, 2000.
(30) Ryde, U.; Olsson, M. H. M.; Pierloot, K. In *Processes and Properties of Biological Systems*; Eriksson, L., Ed.; Elsevier: Amsterdam, 2001; Vol. 9, pp 1−55.
(31) Szilagyi, R. K.; Metz, M.; Solomon, E. I. *J. Phys. Chem. B* **2002**, *106*, 2994−3007.
(32) Guss, J. M.; Bartunik, H. D.; Freeman, H. C. *Acta Crystallogr.* **1992**, *B48*, 790−811.
(33) The equatorial Cu−N, Cu−S and axial Cu−N distances vary from 2.01 to 2.20 Å, 2.16−2.28 Å, and 2.06−2.25 Å, respectively.

Scheme 1

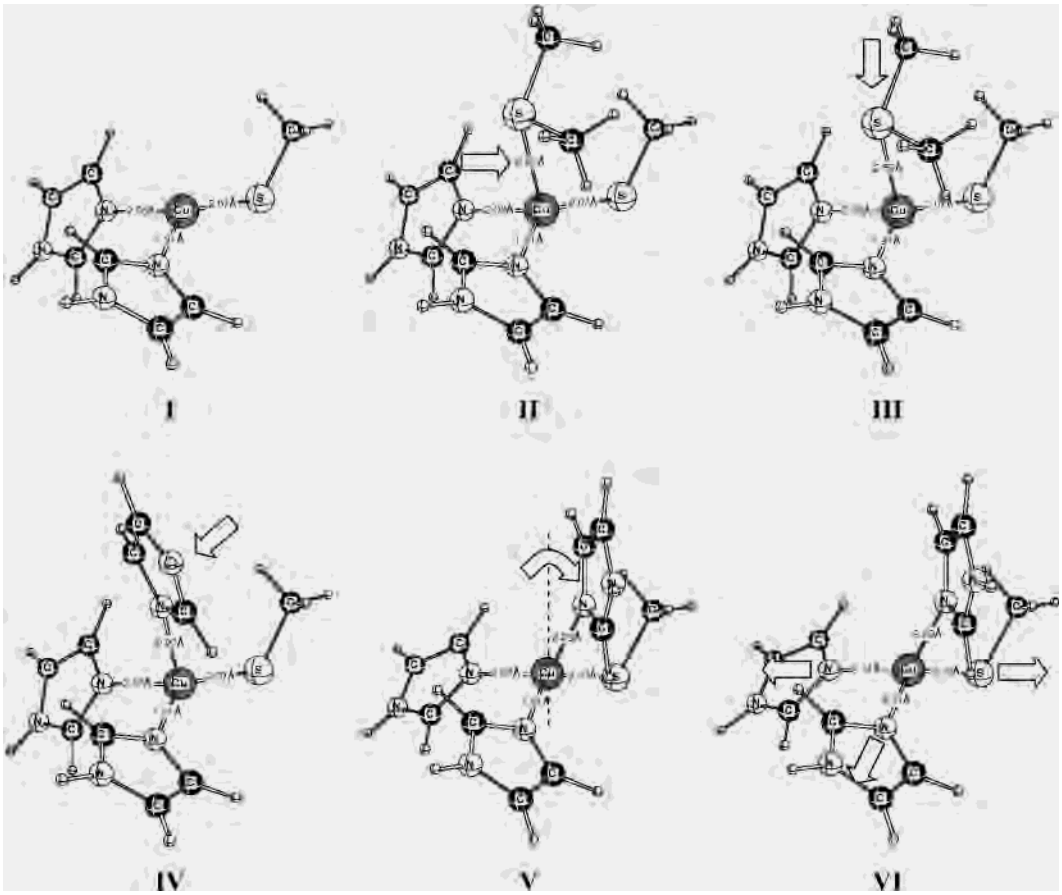

In a systematic analysis of individual internal coordinates defining a distortion coordinate, a series of structures were manually constructed (Scheme 1, vide infra). Structures **I**−**IV** are used to investigate the ligand field strengths of the axial-Met and His ligands in a trigonally distorted tetrahedral environment. Structure **I** lacks the axial ligand, whereas structures **II**−**IV** have an axial-Met at long (2.8 Å as in plastocyanin) and short (2.6 Å as in nitrite reductase) distances and an axial-His at 2.3 Å (as in M121H A.d. azurin), respectively. Structure **V** was derived from **IV** by applying the tetragonal distortion observed in the room-temperature X-ray structure of the M121H A.d. azurin, active site A. The Cu−equatorial ligand bond lengths were fixed to those in **I**−**III**. Structure **VI** corresponds to the experimental geometry of the active site of the RT structure with a longer axial Cu−N(His) bond. Variation in the axial Cu−N(His) distance by 0.04 Å, as found in the M121H A.d. azurin, affects the orbital energies by less than 400 cm^{-1}; therefore, in the systematic DFT study only one variant structure (RT structure with long axial Cu−N(His) bond, HP1-SUA in ref 12) is presented.

Results and Analysis

Characterization of the Axial-His Variant in Laccase. Mutation of Leu513 in the axial position of MtL to His resulted in an enzyme that was green rather than blue in color. The purified variant had a molecular weight of 76 000 on the SDS-PAGE and a UV−visible spectrum with three maxima at 278, 400, and 580 nm. Addition of pyridine, NaOH, and Na-dithionite led to the appearance of two maxima at 556 and 615 nm without the disappearance of the three original peaks, indicating the absence of any heme-like contaminant in the variant MtL preparation.

Metal incorporation was accomplished by in vivo biosynthesis, and as a result the purified protein was not completely loaded with Cu. On average, samples contained 2.35 ± 0.05 Cu/protein (Cu_{total}) distributed among the three Cu sites (vide infra). Incomplete metal incorporation was also observed in previous studies of an axial-His variant of bilirubin oxidase, a close analogue of laccase.[34] Ion-exchange chromatography during protein purification appeared to be sufficient for removing adventitious Cu^{2+}, as confirmed by EPR characterization. One complication of the partially loaded L513H MtL protein is that ∼60% of the Cu is in the reduced (Cu^{1+}) form (1.43 ± 0.04 Cu^{1+}/2.4 Cu_{total}). Spin quantitation of the EPR spectrum revealed that 14% of the Cu is paramagnetic (0.33 spins/2.4 Cu_{total}). Using EPR simulations, we systematically varied the ratio of T1:T2 to determine the distribution of paramagnetic Cu. The best fit to the experimental spectrum was obtained by 1:0.8 ratio of the T1:T2 Cu sites. This ratio could be varied by up to 10% while still obtaining a reasonable fit. Therefore, the T1 Cu site contains 0.18 ± 0.02 spins and the T2 Cu site 0.15 ± 0.02 spins.

The L513H MtL protein could be reduced by standard fungal laccase substrates such as ABTS and hydroquinone and then oxidized upon exposure to O_2, indicating that the

(34) Shimizu, A.; Sasaki, T.; Kwon, J. H.; Odaka, A.; Satoh, T.; Sakurai, N.; Sakurai, T.; Yamaguchi, S.; Samejima, T. *J. Biochem. (Tokyo)* **1999**, *125*.

Table 1. Substrate Specificity of the Leu513His Variant (Measured in 10 mM MES, pH 5.5)

	SGZ		MS		ABTS	
	K_m, μM	k_{cat}, min^{-1}	K_m, μM	k_{cat}, min^{-1}	K_m, μM	k_{cat}, min^{-1}
WT[a]	1.4 ± 0.2	4500 ± 200	2.5 ± 0.7	3200 ± 400	110 ± 20	3800 ± 300
L513H	24 ± 3	70 ± 10	3600 ± 400	18 ± 2	1100 ± 100	160 ± 20
		388 ± 55[b]		100 ± 11[b]		889 ± 111[b]

[a] The data for wild-type MtL are from ref 16. [b] Corrected for the 18% loaded and redox active protein in the L513H variant.

protein was capable of turning over (vide infra). Reduction and reoxidation were monitored by absorption spectroscopy. In all turnover experiments, the protein returned to the same oxidation level (~18% fully oxidized) after turnover, suggesting that a consistent fraction of the protein was fully loaded and redox active (i.e., intact oxidized T1 and T2 and antiferromagnetically coupled T3 sites), whereas the remainder of the protein molecules were incompletely loaded and contained a distribution of reduced Cu among the three sites. A number of experiments were further conducted in an attempt to oxidize the reduced Cu. Ferricyanide was added sequentially (up to a 15× excess) to a sample of 1 mM L513H MtL, and the absorption was monitored over 1.5 h. No change in the 578 nm absorption band was observed, indicating that no T1 Cu was further oxidized under these conditions. Likewise, sequential addition of H_2O_2 (2−10-fold excess) to the protein did not result in an increase in the amount of oxidized T1 Cu (578 nm band) or T3 Cu (330 nm band), as observed by absorption spectroscopy. These experiments suggested that the reduced Cu is likely distributed among protein molecules, which lack appropriate electron-transfer pathways because of partial Cu loading. Because the reduced Cu does not contribute to the spectroscopic properties of the protein and, likewise, because the protein molecules containing absent or reduced Cu do not contribute to protein turnover, spectroscopic and reactivity studies were normalized to allow comparison with wild-type MtL. The L513H MtL data were all normalized by a factor of 1/0.18 to a *fully loaded, oxidized* T1 Cu.

Table 1 summarizes the SGZ, MS, and ABTS-oxidase activities of both L513H and wild-type MtL. Although the L513H variant showed the same optimal pH (pH_{opt}) as the wild type (7 for SGZ and MS, 3 for ABTS), its K_m was 10−1400× higher and k_{cat} was 4−32× lower than those of the wild type. At 20 °C, the inhibitor NaF showed an I_{50} of 0.2 and 6 mM at pH 5.5 and 7.5, respectively, for the variant (with ABTS as the substrate), slightly smaller than those for wild-type MtL (0.3 and 20 mM).

The redox potential of the T1 Cu site in L513H, an important factor for determining catalytic activity, was measured by the poised potential method using the ferri/ferrocyanide redox couple to poise the solution potential. Under these conditions, the redox potential was determined to be 420 ± 20 mV, slightly lower than the value observed for the T1 Cu site in wild-type MtL (450 mV).[35]

EPR Comparison of Wild Type and L513H MtL. The EPR spectra of wild type and L513H MtL as well as the corresponding simulations are presented in Figure 1A. The simulations allow the ground-state spin Hamiltonian parameters for each of the two paramagnetic sites to be extracted. For the T1 Cu, $g_{||}$ increases from 2.201 to 2.240 and the hyperfine coupling constant in the electronic *z* direction, $A_{||}$, increases in magnitude from 87 × 10^{-4} to 102 × 10^{-4} cm^{-1} going from wild type to variant MtL. In the perpendicular region of the T1 Cu, $g_{\perp}$ appears to increase slightly (2.045 for MtL and 2.053 for L513H MtL), whereas $A_{\perp}$ (15 × 10^{-4} cm^{-1} for both) is unchanged by the mutation. It should be noted that small changes in the $g_{\perp}$ region are difficult to detect because of the overlapping T2 Cu EPR signal. For the T2 Cu, $g_{||}$ is 2.247 for both wild type and variant MtL and $A_{||}$ decreases slightly from 185 × 10^{-4} to 180 × 10^{-4} cm^{-1}. In summary, the T1 Cu site is perturbed by the Leu to His mutation, whereas the T2 Cu is relatively unchanged.

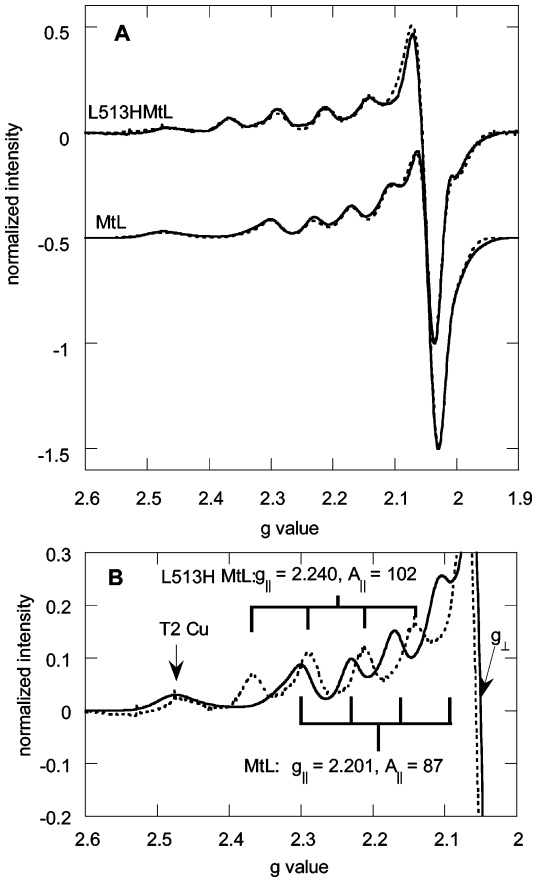

Figure 1. (A) EPR spectra of L513H MtL (solid line, top) and wild type (solid line, bottom) with the respective simulations (dotted line). (B) Expanded scale of the EPR spectra in the parallel region (A values are given in ×10^{-4} cm^{-1}). The instrument parameters were as follows: 9.505 and 9.514 GHz microwave frequency (wild type and variant, respectively), 10.1 mW microwave power, 100 kHz modulation frequency, 20 G modulation amplitude, 500 ms time constant, 500 s sweep time.

(35) Xu, F.; Shin, W.; Brown, S. H.; Wahleithner, J. A.; Sundaram, U. M.; Solomon, E. I. *Biochim. Biophys. Acta* **1996**, *1292*, 303−311.

Given the ligand field expressions for the g values, the increase in $g_{||}$ observed in L513H MtL could result from either a decrease in the ligand field strength or a decrease in covalency. To assess the ligand field contribution, the following simplified expression can be used:[36]

$$\Delta g_{||}(L_{513}H\ MtL) = \frac{\Delta E_{xy}(MtL)}{\Delta E_{xy}(L_{513}H\ MtL)}\Delta g_{||}(MtL) \qquad (1)$$

where $\Delta g_{||}$ is the deviation of the $g_{||}$ value from the spin-only value (2.002) and ΔE_{xy} is the experimental energy of the $xy \rightarrow x^2 - y^2$ ligand field transition. As can be seen from analysis of the optical spectra (vide infra), ΔE_{xy} of L513H MtL is lower than wild-type MtL (12 700 vs 13 160 cm^{-1}), and on the basis of eq 1, this would cause the $g_{||}$ of L513H MtL to increase slightly (from 2.201 to 2.208). To fully account for the experimentally observed increase in $g_{||}$ (2.201 $\rightarrow$ 2.240), the covalency of L513H MtL must also decrease (i.e., the metal character of the singly occupied MO (SOMO) must increase).

The competing factors that influence hyperfine coupling constant are related by the following generalized expression:[36]

$$A = A^{\text{Fermi contact}} + A^{\text{spin dipolar}} + A^{\text{orbital dipolar}} \qquad (2)$$

The experimental increase in $g_{||}$ in L513H MtL alters the $A^{\text{orbital dipolar}}$ contribution to the hyperfine and causes the hyperfine coupling to decrease in magnitude. However, $A_{||}$ in L513H MtL is larger in magnitude than in MtL, and therefore the $A^{\text{Fermi contact}}$ and/or $A^{\text{spin dipolar}}$ contribution must also change upon mutation to overcompensate. For the Fermi contact term to account for the experimental increase in $A_{||}$, there would need to be a *decrease* in 4s mixing into the ground state, and yet the amount of 4s mixing in the ground state of fungal laccases was already found to be negligible.[4] Therefore, $A^{\text{spin dipolar}}$ is the primary factor that contributes to the increase in $A_{||}$ in L513H MtL, where an increase in $A^{\text{spin dipolar}}$ signifies an increase in the metal character of the SOMO in L513H MtL. The magnitude of this increase can be estimated using the experimental g values in the ligand field expressions for the hyperfine coupling and is found to be ~10%.[37] In summary, the increase in g and A values indicates that upon going from the blue Cu site in MtL to the green Cu site in L513H MtL, the covalency of the SOMO decreases by 10%.

The EPR parameters of the T1 Cu in L513H MtL can be compared to those of other green T1 Cu sites. At pH 7, the green T1 Cu in M121H A.d. azurin has $g_{||} = 2.247$ and $A_{||} = 102 \times 10^{-4}$ cm^{-1}.[9] These are quite similar to the parameters for L513H MtL ($g_{||} = 2.240$ and $A_{||} = 102 \times 10^{-4}$ cm^{-1}) and indicate that the ground states of the axial-His variant of azurin and fungal laccase are similar. Alternatively, the EPR parameters of the axial-His variants are quite different from those of the green Cu sites that have Met in the axial position. The $g_{||}$ of NiR is 2.195, whereas the $A_{||}$ is 73×10^{-4} cm^{-1}, which indicates that *the electronic structure of the T1 green Cu site of the axial-His variants is different from that of the axial-Met green Cu proteins.* Electronic structure calculations provide insight into the origin of these differences (vide infra).

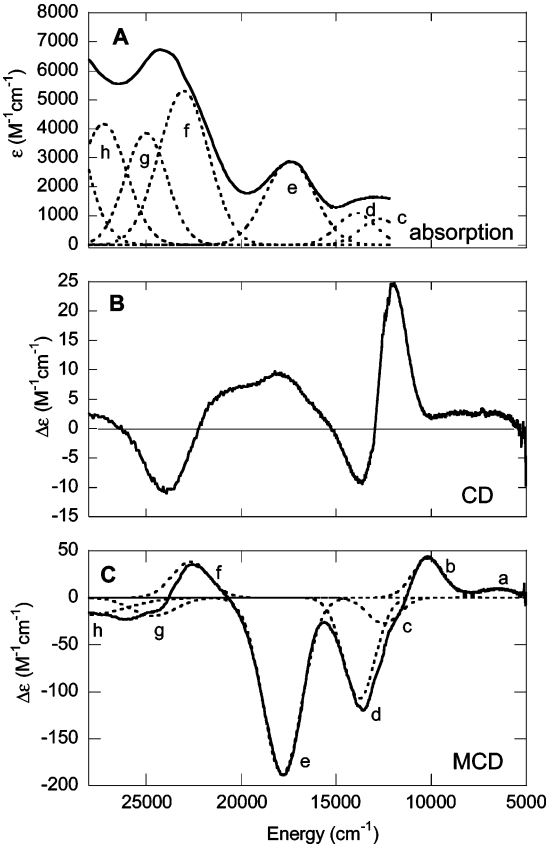

Figure 2. (A) Room-temperature absorption spectrum, (B) Low-temperature (5 K) CD spectrum, and (C) Low-temperature (5 K) MCD spectrum of L513H MtL. The 0 T baseline was subtracted from the 7 T MCD spectrum. The dotted lines in A and C represent the individual Gaussian bands.

Table 2. Summary of Gaussian Bands for L513H MtL

band	energy (cm^{-1})	ϵ (M^{-1} cm^{-1})[a]	C_0/D_0	assignments
a	6550[b]	*c*	*c*	z^2
b	10 150[b]	*c*	*c*	yz
c	12 700	912	−0.0327	xy
d	13 900	1081	−0.1044	xz
e	17 400	2825	−0.0693	Cys π
f	23 000	5300	0.0076	Cys pseudo-σ
g	25 000	3840	−0.0053	His
h	27 200	4175	−0.0046	His

[a] The error in the reported values is at least 10%. [b] The energy of this transition comes from the low-temperature MCD spectrum, whereas the energies of the remaining bands come from the room-temperature absorption spectrum. [c] Not determined because the band was below the detection limit of the absorption spectrometer.

Absorption, CD, and Low-Temperature MCD Spectra of L513H MtL Relative to Those of MtL. The absorption, CD, and MCD spectra of L513H MtL are shown in Figure 2. Simultaneous Gaussian fitting of all three spectra requires eight bands (dashed lines shown in parts A and C of Figure 2) to fit the region between 5000 and 30 000 cm^{-1}. Table 2 lists the energies, experimental extinction coefficients, and

(36) McGarvey, B. R. In *Transition Metal Chemistry*; Carlin, B. L., Ed., 1966; Vol. 3, pp 89−201.

(37) If the experimental g and A values are input into the following equation: $A_{||} = Pd(-\kappa - 4\alpha^2/7 + 3\Delta g_{\perp}/7 + \Delta g_{||}$ and κ is assumed to be the same in MtL and L513H MtL, the difference in metal character ($\alpha^2_{L513H\ MtL} - \alpha^2_{MtL}$) was calculated to be 9.6%.

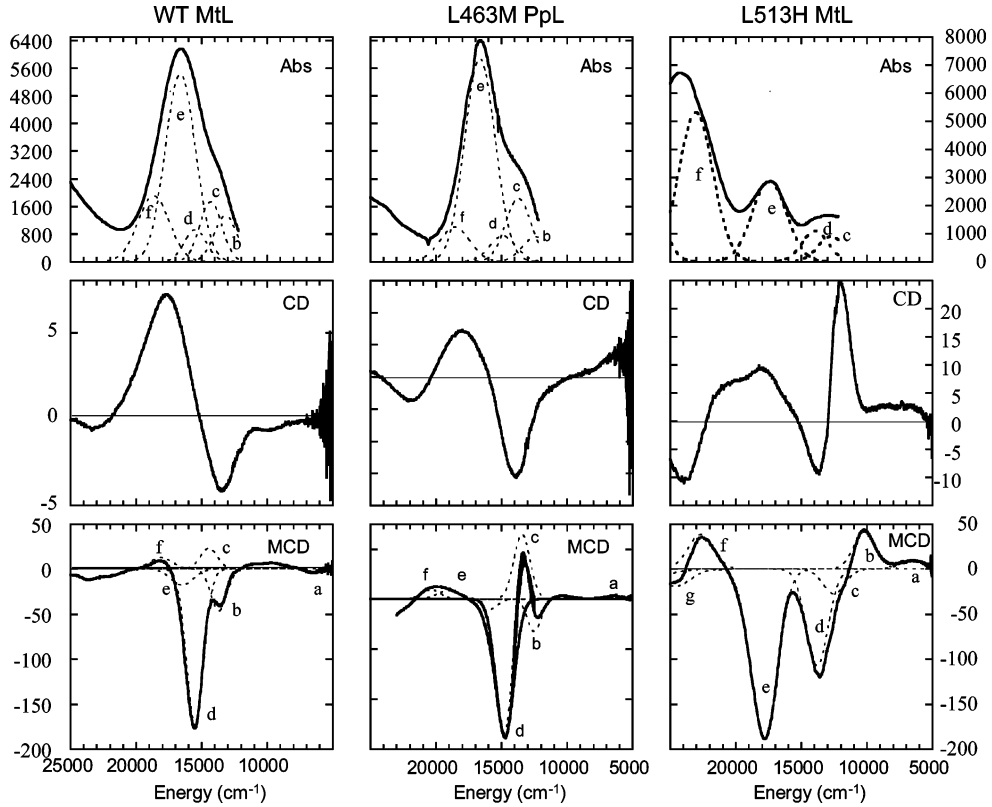

Figure 3. Comparison of the absorption, CD, and MCD of wild-type MtL (left), L463M PpL (middle), and L513H MtL (right). The spectra for wild-type MtL and variant PpL are reproduced with permission from ref 4.

Table 3. Comparison of the Charge-Transfer and Ligand Field Transitions

	transition	MtL[a]	L513H MtL	L463M PpL[a]	M121H A.d. azurin[d]	NiR[b]	Plc[c]
a	z^2	6500	6550	6500		5000	5000
b	*xy*	13 160	10 150 (*yz*)	12 370		11 900	10 800
c	*yz*	14 290	12 700 (*xy*)	13 700		13 500	12 800 ($xz + yz$)
d	*xz*	15 470	13 900	14 880		14 900	13 950 ($xz - yz$)
e	Cys π	16 610	17 400	16 630	16 860	17 550	16 700
f	Cys pseudo-σ	18 650	23 000	18 540	22 800	21 900	18 700

[a] Taken from ref 4. [b] Taken from ref 10. [c] Taken from ref 41. [d] Taken from ref 8.

C_0/D_0 ratios of the individual bands. The C_0/D_0 ratio is a measure of the MCD C-term intensity of a particular transition as compared to its intensity in absorption. C_0/D_0 ratios were calculated using the equation $C_0/D_0 = (kT\Delta\epsilon)/(\mu_B B\epsilon)$, where k is Boltzmann's constant, T is the temperature, μ_B is the Bohr magneton, and B is the magnetic field, and the extinction coefficients are reported in M^{-1} cm^{-1}.[38] In general, the C_0/D_0 helps determine whether a transition is a ligand field or a charge transfer (CT), as ligand field transitions tend to have higher C_0/D_0 ratios.[39]

The three highest-energy transitions (bands f, g, and h) have very low C_0/D_0 ratios and are therefore assigned as CT transitions. Comparison with other blue and green Cu proteins reveals that g and h are likely His (π) → T1 Cu CT transitions, whereas band f is assigned as the Cys pseudo-σ → Cu CT transition.[40] Band e has an ambiguous C_0/D_0 ratio; however, correlation with other T1 Cu proteins reveals that this is the Cys π → Cu CT transition. Bands a−d are attributed to T1 Cu ligand field transitions. These bands can be assigned as excitations from the d_{z^2}, d_{yz}, d_{xy}, and d_{xz} (in order of increasing energy) to the $d_{x^2-y^2}$ ground state based on their signs and relative intensities (in absorption and MCD).[41]

Figure 3 presents a comparison of the absorption, CD, and MCD spectra of wild-type MtL, L463M PpL, and L513H MtL where both the wild type and L463M PpL variant are blue sites and the L513H MtL is a green site. The energies of the individual transitions are summarized in Table 3. Overall, the spectrum of L513H MtL is dramatically different from that of wild-type MtL, suggesting a strong geometric perturbation of the T1 Cu site upon mutation of the Leu to His. As can be seen from Table 3, the ligand field decreases in the axial-His variant. The energy of the d_{z^2} transition is

(38) Piepho, S. B.; Schatz, P. N. *Group Theory in Spectroscopy−With Applications to Magnetic Circular Dichroism*; Wiley & Sons: New York, 1983.

(39) Solomon, E. I.; Hanson, M. A. In *Inorganic Electronic Structure and Spectroscopy*; Solomon, E. I., Lever, A. P. B., Eds.; Wiley & Sons: New York, 1999; Vol. 2, pp 1−130.

(40) It should be noted that attempts were made to obtain resonance Raman on MtLH (excitation λ = 413 and 468 nm). However, the total absorption was too low, and no peaks were observed above the noise.

(41) Gewirth, A. A.; Solomon, E. I. *J. Am. Chem. Soc.* **1988**, *110*, 3811−3819.

about the same in MtL and L513H MtL, but all the other ligand field transitions decrease in energy, with d_{yz} and d_{xz} showing the largest energy change (-3000 and -1600 cm^{-1}, respectively). The ligand field of the axial-Met PpL is between that of the wild type and axial-His variant.

The Cys π and pseudo-$\sigma \rightarrow$ Cu CT transitions in L513H MtL shift to higher energy than that in MtL (by 790 and 4350 cm^{-1}, respectively), and the splitting between the transitions increases ($\Delta = 2040$ cm^{-1} in wild type and 5600 cm^{-1} in this variant). Additionally, there is a significant intensity redistribution of the pseudo-σ and $\pi \rightarrow$ Cu CT transitions ($\epsilon_{\text{pseudo-}\sigma}/\epsilon_{\pi}$ is 0.35 in wild type and 1.87 in the variant). The increase in intensity of the Cys pseudo-σ reflects increased overlap between the Cu $d_{x^2-y^2}$ and the S(Cys) pseudo-σ orbital. Likewise, the decrease in intensity of the Cys $\pi \rightarrow$ Cu CT transition reflects a decrease in overlap of the Cu $d_{x^2-y^2}$ and S(Cys) π orbitals. These changes quantitate the transformation from a blue to a green T1 site and indicate that the His serves as a strong field ligand to the T1 Cu.

The energies and intensities of the Cys pseudo-σ and $\pi \rightarrow$ Cu CT transitions in L513H MtL can be compared to those of M121H A.d. azurin. The absorption spectrum of M121H A.d. azurin at pH 7.0 exhibits two bands, a more intense band at 22 800 cm^{-1} (439 nm) and a weaker band at 16 860 cm^{-1} (593 nm).[9] Resonance Raman profiles revealed that this high pH spectrum was comprised of two species: (1) the green T1 site (labeled T1.5 by the authors), which exhibited two Cys $\rightarrow$ Cu CT absorption transitions at 439 and $\sim$570 nm, and (2) a classic blue Cu site (present as a 25% impurity) that was the primary contributor to the absorption band at 593 nm. This mixture was attributed to changes at the T1 Cu site as a result of hydrogen bonding between His121 and Ser9 (in two different conformations). Decreasing the pH from 7.0 to 3.5 resulted in a significant intensity redistribution of the absorption bands; the 439 nm band decreased in intensity whereas the 593 nm band increased and shifted to slightly lower energy. These changes were attributed to protonation of His121 and dissociation from the T1 Cu. In the L513H MtL variant, the absorption spectrum does not change from pH 7.0 to 3.5, and only a single species contributes to the absorption, CD, and MCD spectra. The fact that only a single species contributes to the absorption spectrum at pH 7.0 may result from the apparent lack of a Ser residue in the immediate vicinity of the T1 Cu and in fungal laccase[42] and therefore the lack of possible hydrogen-bonding interaction with H513. In summary, while the absorption spectra of L513H MtL and M121H A.d. azurin are comparable, the MtL spectrum is not complicated by additional features from a second species.

The spectral properties of the axial-His variant can also be compared to the well-characterized axial-Met green Cu protein, NiR (Table 3). Although the Cys pseudo-σ and $\pi \rightarrow$ Cu CT transitions of both green Cu proteins are at similar energies and have a similar intensity pattern, the average energy of the ligand field transitions of the axial-His fungal laccase variant are significantly lower (10 825 vs 11 325 cm^{-1}).

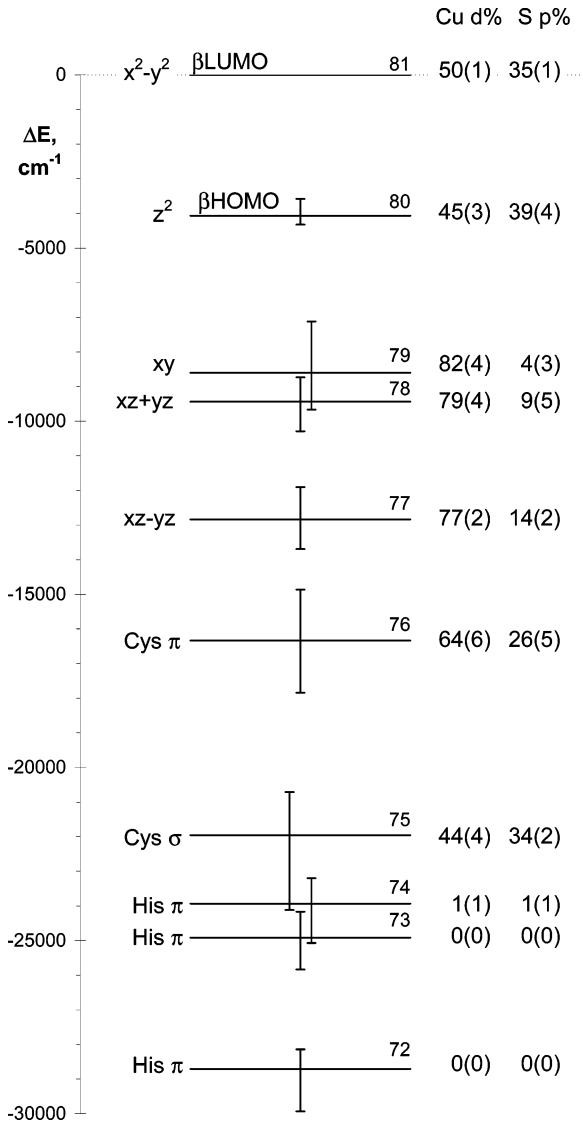

Figure 4. Ground-state orbital energy levels for the axial-His active-site model with Cu 3d and S(Cys) 3p contributions (average deviations corresponding to the variation in the active-site structure[33] are given in parentheses).

Electronic Structure Calculations. Description of the Axial-His Ground-State Wave Function and Comparison to the Classic Blue Cu Site. To model the axial-His active site, density functional calculations were performed using the crystal coordinates of four active-site models (two independent active sites per protein, at two different temperatures) from M121H A.d. azurin (Supporting Information, S2−S5). The total atomic spin densities for the Cu, S(Cys), axial N(His), and equatorial N(His) atoms were calculated by Mulliken Population Analysis to be 54%, 38%, 1%, and 6%, respectively. The spin density is mostly localized on the Cu $3d_{x^2-y^2}$ and S(Cys) 3p orbitals with 11% σ and 27% π character (σ/π ratio of 0.41), respectively. From Figure 4, the βLUMO, which reflects the uncompensated electron density, has similar Cu 3d (50%) and S 3p (35%) characters.

(42) There is no crystal structure available for MtL, but the crystal structure of *Coprinus cinereus* laccase does not show any Ser residues in the immediate vicinity of the T1 Cu.

With this range in the active-site structure,[33] the total atomic spin densities and orbital covalencies vary by only 1%.

The calculated ground-state orbital energy levels and their Cu 3d and S 3p contributions for the axial-His variant are presented in Figure 4. The vertical bars represent the computed shift in the orbital energy on the range of active-site structural variations of the M121H A.d. azurin (Scheme 1, structure **VI**). The largest deviations are found for the d_{xy}, Cys π, and Cys σ levels; however, a change in the order of the levels occurs only in one case.[43] It is worth noting that the agreement between the experimental excitation energies (Table 3, column 6) and the calculated orbital energy differences (Figure 4) is within 500 and 900 cm^{-1} for the Cys π and pseudo-σ transitions, respectively.

In the blue Cu active-site model (Scheme 1, structure **II**, based on the crystal coordinates of plastocyanin), the total atomic Cu and S spin densities are 49% and 42% and the corresponding βLUMO characters are 48% and 38%, respectively. This corresponds to approximately 5% more covalent bonding in **II** than in the axial-His green Cu site (**VI**). The spin density of structure **II** is largely localized on the Cu $d_{x^2-y^2}$ and S(Cys) π orbital, with less than 1% contribution from the S(Cys) σ orbital (contour **II**, top of Figure 5). Thus, the Cu−S(Cys) bond has changed from mixed σ and π in **VI** (σ/π ratio of 0.41) to pure π in **II** (σ/π ratio of 0.03). These results are consistent with a rotation of the $d_{x^2-y^2}$ orbital in the axial-His active site (**VI**) relative to the blue Cu site (**II**), such that the lobe of this metal d orbital is oriented more along the Cu−S(Cys) bond. This rotation derives from the tetragonal distortion of the active-site geometry because of a strong axial interaction (vide infra). Comparison of the orbital energies in the axial-His (Figures 4 and 5, structure **VI**) and blue Cu (Figure 5, structure **II**) models reveals that both the LF and CT transitions decrease in energy in the axial-His active site.

The differences in the electronic structure of the classic blue Cu and axial-His green active sites (Figure 5, structures **II** and **VI**) can be correlated with the experimental differences between the wild type or axial-Met blue Cu sites and the axial-His green Cu variant of fungal laccase (Figure 3 and Table 3). First, the decreased covalency upon going from a blue (**II**, 48% Cu/39% S) to an axial-His green Cu site (**VI**, 50% Cu/36% S) is consistent with the analysis of the experimental g and A values obtained from EPR data for the wild type and axial-Met variant of fungal laccase as compared to the green axial-His variant. Second, the intensity redistribution of the σ and π CT transitions in the absorption spectrum (Figure 3) of L513H MtL as compared to the wild-type spectrum (σ/π ratios of 1.87 vs 0.35, respectively) is qualitatively reproduced by the altered overlap between the Cu $d_{x^2-y^2}$ and S(Cys) π and σ orbitals (Figure 5, SOMO contours of **II** with π overlap vs **VI** with some σ overlap, σ/π ratios of 0.41 vs 0.03, respectively). Quantitative differences likely relate in part to the use of the M121H A.d. azurin structure to correlate with the data on the L513H MtL variant. Third, absorption, CD, and MCD (Figure 3 and Table 3) reveal that the LF transition energies decrease by an average of 1500 cm^{-1} in the L513H MtL as compared to the wild type and axial-Met blue Cu sites, which are also reproduced by the computations.

In summary, a number of differences are observed between the experimental electronic structures of the axial-His and blue Cu active sites, which are reproduced by model calculations. However, as can be seen from the structures used in the calculations (**II** and **VI** in Scheme 1), several internal coordinates change upon going from a classic blue to an axial-His green Cu site. To gain further insight into the geometric origin of the electronic structure changes, a systematic DFT study was performed. Only one structural parameter was altered at each step and the effects of these individual perturbations on the electronic structure were systematically determined in going from a tricoordinate blue Cu (**I**) site to a tetragonal, green Cu (**VI**) site with an axial-His ligand.

Systematic Alteration of Internal Coordinates. Scheme 1 depicts the six structures that comprise this DFT study. These include: **I** (no axial ligand, wild-type fungal laccase-like), **II** (long Met, Plc-like), **III** (short Met, NiR-like without tetragonal distortion), **IV** (axial-His with trigonal pyramidal coordination), **V** (axial-His with tetragonal distortion), and **VI** (M121H A.d. azurin active site, RT structure, long axial Cu−N(His) bond with approximately 0.1 Å longer equatorial Cu−ligand bonds than in **V**). Figure 5 shows the orbital energy changes in going from a trigonal, blue Cu site (**I**) to a tetragonally distorted, green Cu site (**VI**) with an axial-His ligand. In all cases, the five highest energy orbitals have mostly d character. In general, the change in the d−d energies going from **I** (no axial ligand, trigonal geometry) to **VI** (His-axial ligand, tetragonal geometry) reproduces the experimental trend of wild type to the His variant of fungal laccase (vide supra).

The strength of the axial ligand and its effect on the electronic structure can be quantitated by the comparison of structures **I**−**IV**. In these model complexes, the Cu $3d_{x^2-y^2}$ orbital-based βLUMO has approximately 37% S(Cys) character, which is pure π. The energy of the βHOMO, which has mainly $3d_{z^2}$ character, is an indicator of the axial ligand field strength. It is most stabilized in **I**, where the axial ligand is absent. The presence of an axial-Met at 2.82 Å (**II**) and at 2.59 Å (**III**) destabilizes the βHOMO by approximately 3000 and 4000 cm^{-1}, respectively. In **IV**, the destabilization is about 3700 cm^{-1}, indicating a decreasing order of axial ligand strength of S(Met) at 2.59 Å (**III**) > N(His) at 2.28 Å (**IV**) > Met at 2.82 Å (**II**). It is worth noting that the variation of the Cu−axial ligand distance has only a small effect on the energy of the other Cu 3d orbitals and no effect on the orbitals related to Cu−S(Cys) and Cu−N(His) bonding.

Increased axial ligand strength in **IV** relative to **II** or **I** is accompanied by additional structural changes (due to an increased Jahn−Teller force leading to a coupled distortion, vide infra), which are taken into account by going from **IV**

(43) The active-site structure labeled as HP2-SUB in ref 12 has the His π (MO74) at higher energy than that of the Cys σ (MO75), whereas this order is reversed in the other three structures (HP1-SUA, HP1-SUB, HP2-SUA) in ref 12, as shown in Figure 4.

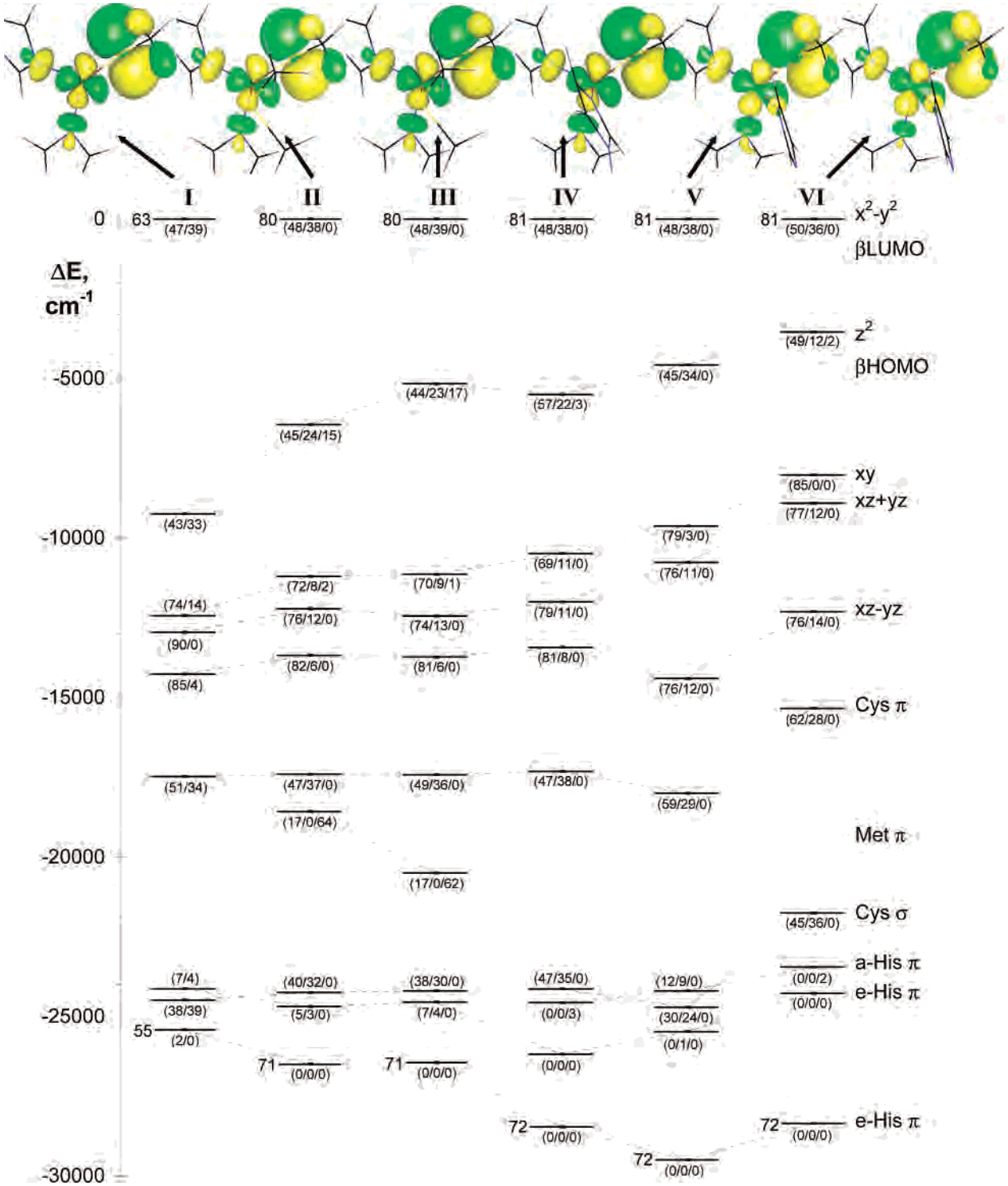

Figure 5. Effect of systematic alteration of internal coordinates on the molecular orbital energy levels (numbers in parentheses are the Cu 3d/S(Cys) 3p/axial S(Met) 3p or N(His) 2p percentages of orbital character).

to **V**. Upon the tetragonal distortion in **V**, the βLUMO gains about 11% σ character (vide supra). This qualitatively reproduces the experimental observation of an altered orbital overlap (decreased π and increased σ) between the Cu $3d_{x^2-y^2}$ and S(Cys) 3p orbitals in the axial-His variant. In addition, the tetragonal distortion strongly affects the d-manifold splitting and the S(Cys) π orbital position. The energy difference between the βLUMO and d_{xz-yz} orbital increased by more than 1000 cm^{-1} as the result of the tetragonal distortion. The Cys π orbital is stabilized by approximately the same amount. The distortion has only a slight effect on the Cys pseudo-σ orbital and a small effect on the equatorial His orbitals as expected from the identical Cu−equatorial ligand distances between **IV** and **V**.

The increase in the LF transition energies upon going from **IV** (or **II**) to **V** is opposite to the behavior observed for the axial-His green Cu site relative to that for the classic blue Cu site. However, as the equatorial distances are allowed to

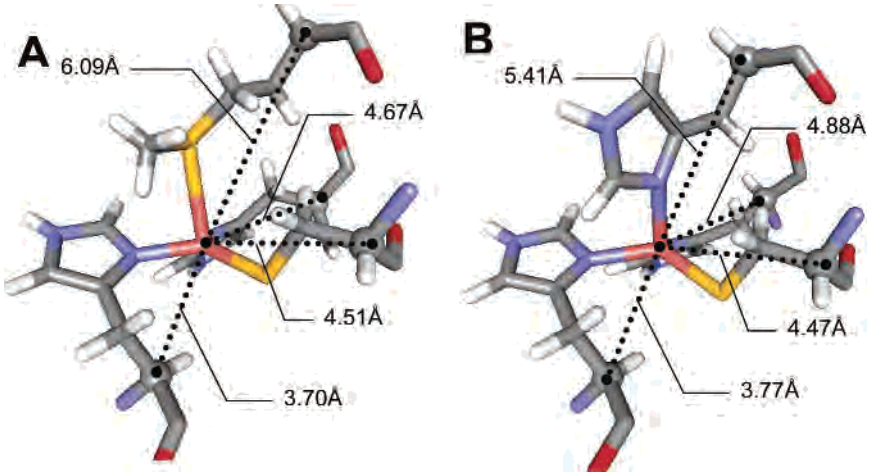

Figure 6. Blue Cu (A) and M121H A.d. azurin, RT, long axial Cu−N(His) bond (B) active-site geometries with Cu−αC(backbone) distances.

relax into their experimental positions (in the case of **VI**, elongation by ca. 0.1 Å relative to **V**), the covalency decreases by 5% and the orbital levels shift to higher energies, resulting in lower d−d splitting energies (12 300 cm^{-1} in **VI** compared to 14 500 cm^{-1} in **V**) in agreement with experiment.

Discussion

This study presents an experimental analysis of the electronic structure of an axial-His green Cu variant in fungal laccase. Changing the noncoordinating, axial-Leu to His causes significant changes in the electronic structure of the T1 Cu site. Overall, the ground-state, $d_{x^2-y^2}$-based SOMO becomes less covalent (i.e., has more metal character), the ligand field decreases, and the interaction between the Cu and S(Cys) is altered such that the overlap of $d_{x^2-y^2}$ with Cys π orbital decreases while its overlap with the Cys pseudo-σ increases.

To gain insight into the geometric origin of the electronic structural changes, spectroscopically adjusted DFT calculations were performed on the crystallographically characterized axial-His variant of azurin (M121H A.d. azurin) to model the electronic structures of the axial-His green Cu vs blue Cu site. These calculations reproduced the experimental trends observed upon going from wild-type MtL to L513H MtL, including the decreased covalency of the His variant, rotation of the $d_{x^2-y^2}$ orbital relative to the Cu−S(Cys) bond giving increased σ character, and the shift of the d−d transitions to lower energy. The associated DFT study of a systematic perturbation of internal coordinates provides insight into the structural origin of these electronic changes. We have found that *the tetragonal distortion in going from **IV** to **V** is the dominant effect* in going from the wild-type MtL to the L513H MtL variant. This leads to a σ overlap between the Cu and S(Cys) orbitals and to the green color. In addition, this distortion decreases the covalency of the site. However, this increases the energy of the LF transitions, which is opposite to what is observed in the MCD experiment. These energies are decreased by the elongation of the equatorial Cu−N(His) bonds, which lowers the ligand field strength of the axial-His green site.

The EPR parameters of L513H MtL compare well with M121H A.d. azurin but show significant differences when compared to the parameters of the green Cu sites of NiR and CBP. Increased g and A values (L513H MtL $g_{||} = 2.240$, $|A_{||}| = 102 \times 10^{-4}$ cm^{-1} vs NiR $g_{||} = 2.195$, $|A_{||}| = 73 \times 10^{-4}$ cm^{-1}) can now be understood as directly reflecting the decrease of LF transition energies in the green variant of L513H MtL compared to NiR. This leads to increased spin orbit coupling into the ground state for the His variant, thus leading to larger $g_{||}$ values. The larger $g_{||}$ value would increase the orbital dipolar contribution ($A^{\text{orbital dipolar}}$) to hyperfine coupling constant, which opposes the spin dipole contribution ($A^{\text{spin dipolar}}$) and will lower $A_{||}$ (vide supra in eq 2). However, the covalency of the ground state of the L513H MtL site is also decreased, contributing to the net-increased $A_{||}$. Several factors explain the differences between the nature of the axial-Met and axial-His green Cu sites. The strength of the axial ligands in both **III** and **VI** are greater than in **I,** which induces a tetragonal distortion and shifts the LF transitions to higher energy. In the His variant site (**VI**), the axial ligand donates less charge than the short axial-Met (**III**) of NiR because of the difference in overlap of the Cu 3d with the N 2p relative to the S 3p-orbitals. Thus, the tetragonal distortion is less in the His green site relative to the NiR (vide infra). Furthermore, the equatorial bond lengths of the axial-His variant are more elongated (by 0.08−0.11 Å) than the axial-Met counterparts, which decreases the LF strength and shifts the d → d transitions to lower energy.

The elongation of the equatorial Cu-ligand bonds could be due to increased ligand−ligand steric repulsion for the bulkier axial-His as compared to that of the more flexible Met. This trend is reflected in the shorter axial Cu−αC(His) distance of 5.41 Å in M121H A.d. azurin relative to those of Plc (6.09 Å), whereas the equatorial Cu−αC(Cys) and Cu−αC(His) distances (4.51, 3.77, and 4.88 Å versus 4.47, 3.70, and 4.67 Å, respectively, Figure 6) remain relatively unchanged.

A coupled distortion coordinate (shorter axial ligand, longer Cu−S(Cys) and tetragonal distortion) connects the blue Cu in Plc and the green Cu in NiR. The overall structure of the axial-His green Cu site is between that of the Plc and

NiR sites, closer to NiR. The strength of the axial ligand reflected by the orbital energy of the βHOMO (i.e., **III** > **IV** > **II** in Figure 5) is also consistent with this trend. The characteristic angle (φ) between the N(His)−Cu−N(His) and S(Cys)−Cu−S(Met)/N(His) planes, which depicts the extent of tetragonal distortion, is 82° in Plc, 61° in NiR, and averages to 66° in the M121H A.d. azurin active site. The out-of-plane distance (δ) of the Cu atom from the plane of equatorial N and S atoms is 0.36 Å in Plc, 0.63 Å in NiR, and 0.58 Å in M121H A.d. azurin. The calculated S(Cys) character also shows a similar trend as the σ character increases from less than 1% in blue Cu to 11% in M121H A.d. azurin and 32% in NiR.[44]

The change of electronic structure of the axial-His green Cu variant correlates with the change in reactivity (Table 1). The rate-limiting step in the turnover of multicopper oxidases is the reduction of the T1 site. According to Marcus theory,[45] this is dependent on a number of factors including redox potentials (E_o). Replacement of an open axial coordination site in the wild-type fungal laccase with a His donor ligand, coupled with the tetragonal distortion of the T1 site, would be expected to stabilize the oxidized site, hence lower E_o. In the L513H variant, the redox potential of the T1 site decreases by 30 mV as compared to the wild-type MtL This decrease, which is smaller than in azurin where the Met → His substitution lowers the potential by approximately 100 mV,[9] can, however, account for an approximately 10-fold[46] decrease of k_{cat} in Table 1.

In summary, spectroscopic studies on the L513H MtL provide a detailed description of the electronic structure of an axial-His green Cu site. Relative to the classic blue Cu site in plastocyanin, there is a change from π to σ bonding with the Cys ligand resulting in the color change, a decrease in the covalency of the SOMO, and a decrease in the ligand field transition energies. Although the π to σ bonding change is also present in green sites such as NiR, the latter sites exhibit LF transitions that shift to higher energy (as compared to blue Cu). This difference can be understood in terms of the competing factors that influence the ligand field around the green Cu site. In NiR, the tetragonal distortion dominates, shifting the d−d bands to higher energy, whereas in the L513H MtL variant, elongation of the equatorial ligands reduces the ligand field around the Cu center and shifts the d−d bands to lower energy. The increased charge donation of the axial-His ligand (and associated tetragonal distortion) in green Cu compared to the axial-Met ligand in blue Cu contributes to the lower redox potential and, hence, to the difference in reactivity of these sites.

Acknowledgment. We thank Kyle Duke and Stephen H. Brown for helpful discussions and contributions to this work. The work was supported by NIH DK31450 and NSF CHE-9980549 to E.I.S. A.E.P. was a Franklin Veatch Memorial Fellow.

Supporting Information Available: Structures of atomic coordinates of computational models used in Figure 4 and Scheme 1 (PDF). This material is available free of charge via the Internet at http://pubs.acs.org.

IC026099N

(44) Basumallick, L.; Szilagyi, R. K.; Scholes, C. P.; Solomon, E. I. In preparation.
(45) Marcus, R. A.; Sutin, N. *Biochim. Biophys. Acta* **1985**, *811*, 265.
(46) Machonkin, T. E.; Quintanar, L.; Palmer, A. E.; Hassett, R.; Severance, S.; Kosman, D. J.; Solomon, E. I. *J. Am. Chem. Soc.* **2001**, *123*, 5507−5517.